JMEPEG (2012) 21:516–523
DOI: 10.1007/s11665-011-9936-x

1059-9495/$19.00

The Effect of Deformation Heating on Restoration and Constitutive Equation of a Wrought Equi-Atomic NiTi Alloy

A. Ahadi, A. Karimi Taheri, K. Karimi Taheri, I.S. Sarraf, and S.M. Abbasi

(Submitted November 1, 2010; in revised form March 15, 2011)

In this study, a set of constitutive equation corrected for deformation heating is proposed for a near equi-atomic NiTi shape memory alloy using isothermal hot compression tests in temperature range of 700 to 1000 °C and strain rate of 0.001 to 1 s^{-1}. In order to determine the temperature rise due to deformation heating, Abaqus simulation was employed and varied thermal properties were considered in the simulation. The results of hot compression tests showed that at low pre-set temperatures and high strain rates the flow curves exhibit a softening, while after correction of deformation heating the softening is vanished. Using the corrected flow curves, the power-law constitutive equation of the alloy was established and the variation of constitutive constants with strain was determined. Moreover, it was found that deformation heating introduces an average relative error of about 9.5% at temperature of 800 °C and strain rate of 0.1 s^{-1}. The very good agreement between the fitted flow stress (by constitutive equation) and the measured ones indicates the accuracy of the constitutive equation in analyzing the hot deformation behavior of equi-atomic NiTi alloy.

Keywords activation energy, constitutive equation, deformation heating, NiTi

1. Introduction

Owing to their unique properties such as superelasticity, shape memory effect, and biocompatibility the NiTi shape memory alloys have been exploited for myriad medical and industrial applications (Ref 1, 2). In NiTi alloys, because of the good workability of the high temperature phase (B2) these alloys are hot worked during the initial stages of manufacturing with the purpose of breaking the cast structure (Ref 3) or achieving a desired dimension. Therefore, an insight into the mechanical properties of the alloy related to the forming process variables such as temperature and working rate is of great importance. During the last decades, with the evolution of powerful finite element packages the precise analysis of forming processes has become feasible. It has been reported that the accuracy of the results relies on the input data introduced to the package such as boundary conditions or constitutive equation that determines the flow behavior of the material (Ref 4). The accuracy of the constitutive equation is customarily influenced by the correctness of its constants which are derived from many tests such as compression, tension, and torsion. In these tests, the temperature of the specimen being deformed rises with respect to the imposed strain rate and thermal properties. It is well known that for the materials with high strength, low specific heat, and low thermal conductivity adiabatic heating is a major source of uncertainty in dynamic test data (Ref 5). Moreover, when the temperature rises, the flow curve does not reflect the real flow behavior of the material at a fixed temperature leading to the introduction of notable deviations in constitutive constants. In this case, the flow curves should be corrected, i.e., the effect of temperature rise during the tests should be eliminated to derive the constitutive constants at a fixed temperature.

Goetz and Semiatin (Ref 6) reported a maximum adiabatic temperature rise of about 110 °C for TiAl alloy during hot compression at temperature of 1093 °C and strain rate of 0.1 s^{-1}. Bruschi et al. (Ref 7) reported an average temperature rise of about 41 °C during hot compression of Ti-6Al-4V alloy at temperature of 800 °C and strain rate of 1 s^{-1}. Zhang and Zhang (Ref 8) stated a temperature rise of about 60 °C for a Ni-rich Ni-Ti alloy during nonisothermal hot compression at temperature of 700 °C and strain rate of 7.8 s^{-1}. It is observed that Ti alloys undergo a considerable temperature rise during hot compression, suggesting deformation heating as a feasible mechanism of softening. In this case, the hot flow curves do not reflect the real flow behavior of the alloy leading to considerable errors in the validity of constitutive constants. Therefore, the effect of temperature rise should be eliminated from the flow curves.

This study was aimed to evaluate the effect of temperature rise on the flow behavior of a near equi-atomic NiTi shape memory alloy to propose a constitutive equation devoid of the effect of deformation heating. Moreover, a temperature-dependent relationship for heat capacity is employed to achieve the more precise results. The results are then compared with those reported on previous publications about hot deformation of Ni-rich alloys.

A. Ahadi and **I.S. Sarraf**, Department of Metallurgy, Saveh-Branch, Islamic Azad University, Saveh, Iran; **A. Ahadi, A. Karimi Taheri,** and **I.S. Sarraf**, Department of Materials Science and Engineering, Sharif University of Technology, Azadi Avenue, Tehran, Iran; **K. Karimi Taheri**, Department of Mechanical and Aerospace Engineering, Science and Research-Branch, Islamic Azad University, Tehran, Iran; and **S.M. Abbasi**, KNT University, Tehran, Iran. Contact e-mails: aslan25253@gmail.com and ktaheri@sharif.ir.

2. Experimental Procedure

In this investigation, a near equi-atomic NiTi shape memory alloy produced by vacuum induction melting (VIM), homogenized at 1050 °C for 2 h followed by a hot rolling at this temperature to a total thickness reduction of 62% was used. Table 1 shows the chemical composition of the alloy. A plate of the alloy with dimensions of $400 \times 60 \times 11.7$ mm^3 was annealed at 850 °C for 2 h in argon atmosphere to eliminate the prior hot working effects. The cylindrical specimens with height of 15 mm and diameter of 10 mm were machined from the longitudinal direction of the plate. The tests were carried out using an Instron 8500 machine at strain rates ranging from 0.001 to 1 s^{-1} and temperatures between 700 and 1000 °C in 100 °C intervals up to true strain of 0.9. In order to obtain a uniform temperature distribution the specimens were held at the preset temperature for 550 s. Mica flakes were embedded at the interfaces of the specimen and anvils to reduce the frictional effect during the hot compression tests. The force-displacement data were used to calculate the true stress and true strain for obtaining the flow curves. Afterward, the effect of friction was eliminated from the stress-strain flow curves and a least-square approach was employed for the derivation of constitutive equation constants. In order to assure the validity of simulations in determining the temperature rise during the tests, a small hole with diameter of 0.15 mm was drilled at mid-height through the center of four cylinders and a thermocouple with a diameter of 0.1 mm was inserted to capture the temperature changes during the tests. Figure 1 shows a sketch of the sample and testing fixture during the hot compression tests.

Table 1 Nominal composition of the alloy (at.%)

Element	Ti	Ni	O	C
Atomic percent	50.04	Bal.	<0.05	<0.02

3. Simulation of Hot Compression Test

In this study, a commercial finite element software package, ABAQUS™ version 6.7 was used to simulate three dimensional isothermal hot compression tests. Since the tests were isothermal, a completely adiabatic with nonisothermal conditions in the specimen, but no heat transfer to the dies and environment was assumed for simulations. The specimen was modeled as a deformable 3D part consisted of 3400 C3D8RT elements. The anvils were modeled as analytical rigid parts. A Young's modulus of 70 GPa, density of 6.45 g/cm^3, thermal expansion of 11×10^{-6} degree^{-1} (Ref 9), and thermal conductivity of 0.18 W/cm·°C were used as the alloy constants. Moreover, the following function was used to relate the change of heat capacity with temperature (Ref 10):

$$C_p = 3R\left(\frac{346}{T}\right)^2 \frac{\exp(346/T)}{(\exp(346/T)-1)^2} + 6.33 \times 10^{-3} T \ (\text{J/mol} \cdot \text{degree}) \quad 481 < T < 1000 \ (^\circ\text{C})$$

A general contact algorithm was used to ensure that proper contact conditions are efficiently enforced. In order to determine the flow behavior of the material prior to the correction of deformation heating, a power-law constitutive equation that will be proposed in section 6.1 was introduced using an Abaqus sub-routine.

4. Eliminating the Effect of Friction and Obtaining the Flow Curves

With the progression of compression test, the interface between the sample and the anvils increases and the effect of friction becomes more pronounced especially at strains of

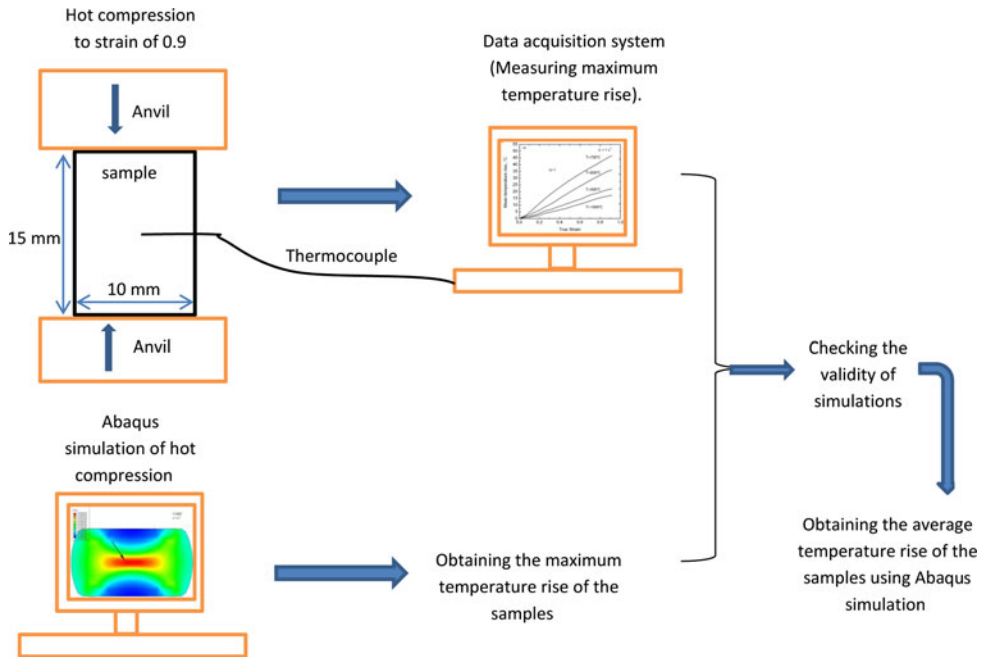

Fig. 1 A sketch of the sample and testing fixture during the hot compression

higher than 0.7 (Ref 11). In this investigation, the flow curves were modified using the following relationship (Ref 12):

$$\bar{\sigma} = \frac{\bar{\sigma}_a}{1 + \frac{2}{3\sqrt{3}} m \frac{R_0}{H_0} \exp\left(\frac{3\bar{\varepsilon}}{2}\right)} \quad \text{(Eq 1)}$$

where R_0 and H_0 are the initial radius and height of specimen, respectively, m is the constant friction factor, $\bar{\sigma}$ the corrected true stress, and $\bar{\sigma}_a$ and $\bar{\varepsilon}$ are the true stress and true strain corresponding to homogenous deformation, respectively. The latter parameters are calculated as:

$$\bar{\sigma}_a = \left| \frac{ph}{\pi R_0^2 H_0} \right| \quad \text{(Eq 2)}$$

$$\bar{\varepsilon} = \ln\left(\frac{H_o}{H}\right) \quad \text{(Eq 3)}$$

where p and h are the current force and height of the specimen, respectively.

The constant friction factor was measured using the following relationship (Ref 13):

$$m = \frac{(R/H)}{(4/\sqrt{3}) - (2b/3\sqrt{3})} \quad \text{(Eq 4)}$$

where

$$b = 4\frac{\Delta R\ H}{R\ \Delta H}$$

and

$$R = R_0\sqrt{\frac{H_0}{H}}$$

ΔR is the difference between the maximum radius (R_{M}) and top radius (R_{T}) of the compressed cylinder, $\Delta R = R_{\mathrm{M}} - R_{\mathrm{T}}$, and $\Delta H$is the difference between the initial height (H_0) and height of the cylinder after compression (H), $\Delta H = H_0 - H$. In practice, it is difficult to measure the top radius of the compressed cylinder. Najafizadeh and Ebrahimi have proposed the following equation for the top radius of the compressed cylinder:

$$R_{\mathrm{T}} = \sqrt{3\frac{H_0}{H}R_0^2 - 2R_{\mathrm{M}}^2} \quad \text{(Eq 5)}$$

Now, by putting the values of m in Eq 1 the flow curves related to the friction-free state can be plotted.

5. Constitutive Equations

Constitutive equations are employed to relate the flow stress of the material to hot deformation variables such as strain, strain rate, and deformation temperature. For this purpose, three types of equations are generally used to model the flow curves during hot working. Hyperbolic sine law constitutive equation is the most widely used to relate the flow stress to deformation parameters (Ref 14, 15):

$$A'[\sinh(\alpha\sigma)]^n = \dot{\varepsilon}\exp\left(\frac{Q}{RT}\right) \quad \text{(Eq 6)}$$

where $\dot{\varepsilon}$ is the strain rate (s^{-1}), σ the flow stress (MPa), Q the activation energy of hot deformation (kJ/mol), R the universal gas constant (J/mol·K), T the absolute temperature (K), A', n, and α are the material constants. At low stress levels $\sinh(\alpha\sigma) \cong \alpha\sigma$ and Eq 6 can be rewritten as:

$$A\sigma^n = \dot{\varepsilon}\exp\left(\frac{Q}{RT}\right) \quad \text{(Eq 7)}$$

Moreover, the Zener-Holloman parameter that embraces the two hot working variables, i.e., $\dot{\varepsilon}$ and T is defined as:

$$Z = \dot{\varepsilon}\exp\left(\frac{Q}{RT}\right) \quad \text{(Eq 8)}$$

In order to obtain the constitutive constants a least-square method was employed using the friction-free hot flow curves. By taking the natural logarithm of Eq 7 we get:

$$\ln(A) + n\ln(\sigma) = \ln(\dot{\varepsilon}) + \frac{Q}{RT} \quad \text{(Eq 9)}$$

The value of n can be obtained from the average slope of the lines in $\ln(\dot{\varepsilon}) - \ln(\sigma)$plot. By differentiating Eq 9 with respect to $1/T$ and rearranging we get:

$$\left(\frac{\partial \ln(\dot{\varepsilon})}{\partial T^{-1}}\right)_{\sigma} = \left(\frac{\partial \ln(\dot{\varepsilon})}{\partial \ln(\sigma)}\right)_{\mathrm{T}} \left(\frac{\partial \ln(\sigma)}{\partial T^{-1}}\right)_{\dot{\varepsilon}} = -\frac{Q}{R} \quad \text{(Eq 10)}$$

where

$$\frac{\partial \ln(\sigma)}{\partial T^{-1}} = S$$

therefore $Q = -nRS$.

Consequently, by substituting the value of Q and other deformation parameters into Eq 8 the Z parameter is calculated. From the intercept and slop of the line in $\ln(Z) - \ln(\sigma)$ plot the values of A and n can be obtained. Repeating the calculations at each selected strain the variation of constitutive constants as a function of strain is obtained.

6. Results and Discussion

6.1 Constitutive Equation of Equi-Atomic NiTi Prior to Correction

In order to relate the constitutive constants with strain a fourth-order polynomial was used. The following fitted polynomials can be used for the equi-atomic NiTi prior to the correction of deformation heating:

$$n = -4.71\varepsilon^4 + 8.43\varepsilon^3 - 3.91\varepsilon^2 + 1.93\varepsilon + 5.75 \quad \text{(Eq 11)}$$

$$Q = -479.08\varepsilon^4 + 901.64\varepsilon^3 - 628.74\varepsilon^2 + 250.5\varepsilon + 190.95 \quad \text{(Eq 12)}$$

$$\ln(A) = -19.78\varepsilon^4 + 37.37\varepsilon^3 - 35.55\varepsilon^2 + 13.96\varepsilon - 8.75 \quad \text{(Eq 13)}$$

Figure 2 shows the comparison between the experimental and the fitted hot flow curves obtained by employing Eq 7 and 11-13. It is seen that the proposed constitutive equations satisfactorily describe the hot flow behavior of the alloy prior to the correction of deformation heating. Obviously, at low deformation temperatures and strain rate of 1 s^{-1} both of the fitted and the experimented flow curves undergo a maximum stress, known as peak stress, followed by a continual decrease

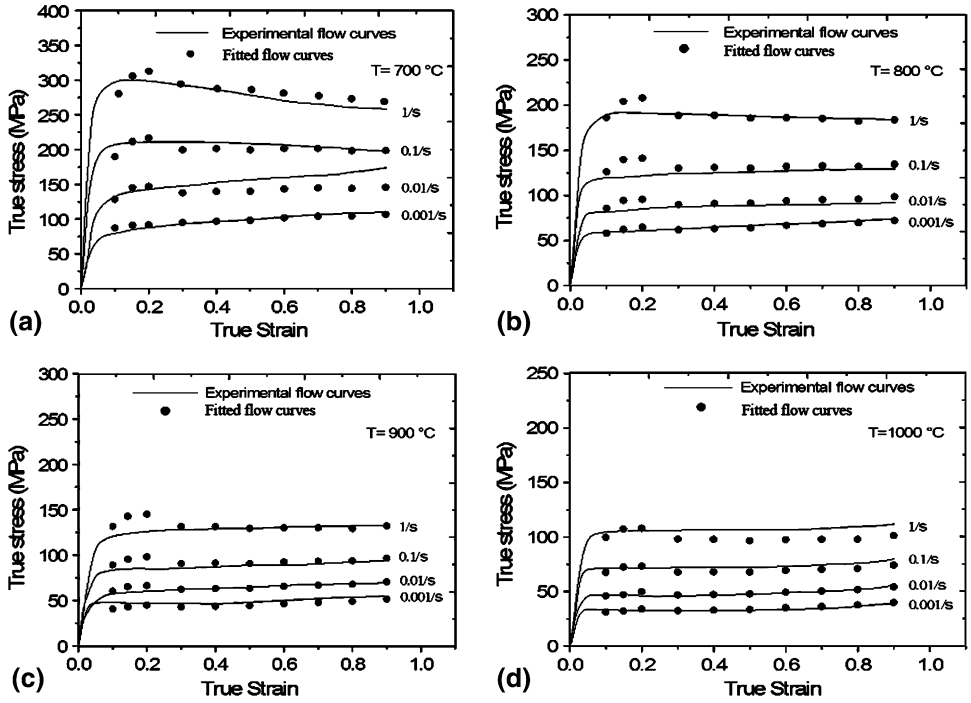

Fig. 2 Comparison between the fitted flow curves and the measured ones for (a) 700 °C, (b) 800 °C, (c) 900 °C, (d) 1000 °C

in the value of stress. However, the fitted flow curves represent this behavior at any other temperatures and strain rates. According to the literatures, the occurrence of flow softening in the hot flow curves is attributed to metallurgical processes such as dynamic recrystallization (DRX) (Ref 16, 17). In general, dynamic recrystallization has been frequently observed at low strain rates where there is enough time for the DRX grains to nucleate and grow (Ref 18, 19). On the other hand, deformation heating is a major source of softening for materials with low thermal properties and high strength such as Ti-alloys. During the hot working of these alloys, the temperature of the deforming body increases with respect to the strain rate and pre-set temperature. At high strain rates, because of the higher strength of the material more power is needed to deform the alloy. Moreover, there is not enough time for the generated heat to be dissipated to the environment leading to significant temperature rise during the tests.

6.2 Correction of Deformation Heating and Flow Behavior

The first step for eliminating the effect of deformation heating is to determine the average temperature rise of the cylindrical specimens during compression. It is generally understood that, during deformation 95% of the plastic deformation is converted to heat and only 5% remains in the material as stored energy (Ref 7). At strain rates of 10^{-3} s^{-1} and lower, the amount of generated heat is not notable since there is enough time for the generated heat to conduct away so that the test is isothermal. The temperature rise due to plastic deformation can be calculated by the following equation (Ref 6):

$$\Delta T = \frac{\eta\, 0.95 \int \sigma d\varepsilon}{(\rho C_p)} \qquad \text{(Eq 14)}$$

where η is the adiabatic correction factor, $\int \sigma d\varepsilon$ the amount of work done by deformation being equal to the area under the stress-strain curve, ρ the density, C_p the specific heat, 0.95 the fraction of mechanical work converted to heat, and ρC_p as the heat capacity. The adiabatic correction factor, η, changes between zero and one for an ideal nonisothermal test condition and completely adiabatic test, respectively. η is expressed as:

$$\eta = \frac{\Delta T_{\text{Actual}}}{\Delta T_{\text{Adiabatic}}} \qquad \text{(Eq 15)}$$

Generally speaking, it has been assumed that η is only dependent on strain rate and independent of strain. However, η varies with strain, temperature, thermal properties of the workpiece and tooling, and the heat transfer coefficients at the interfaces (Ref 20). In this study, η was assumed to be equal to 1 since ideal isothermal condition was assumed in the simulations and no heat transfer with the surrounding environment was considered, i.e., $\Delta T_{\text{Actual}} = \Delta T_{\text{Adiabatic}}$. Figure 3 shows the maximum temperature rise of the specimens at different pre-set temperatures and strain rate of 1 s^{-1}, illustrating a very good agreement between the experimental and the simulated results. Moreover, referring to this figure it is possible to claim that the assumption of an ideal isothermal hot compression in the simulations is likely to be justified. In Fig. 4, the average temperature rise of the specimens obtained from Abaqus simulations is presented. It is seen that the average temperature rise of equi-atomic NiTi during hot compression at high strain rates and low temperatures is significant, being consistent with other researches on Ti-alloys (Ref 6-8). It is worth noting that in this study a temperature-dependent heat capacity for NiTi alloy was considered in the simulations, which gives rise to very precise simulation of temperature rise during deformation. This study may be considered as an extension of the deformation heating on NiTi alloy, (Ref 8), in which a relationship between heat capacity and temperature has not been taken into account. Comparing Fig. 3 and 4 it is conspicuous that the average temperature rise

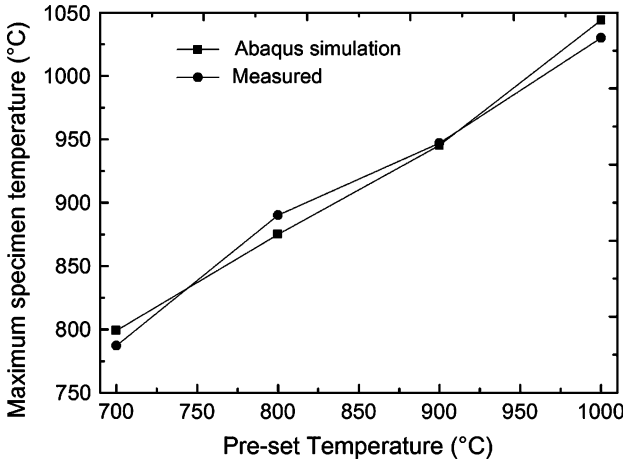

Fig. 3 Maximum temperature rise (center of the specimens) at strain rate of 1 s^{-1} and different temperatures

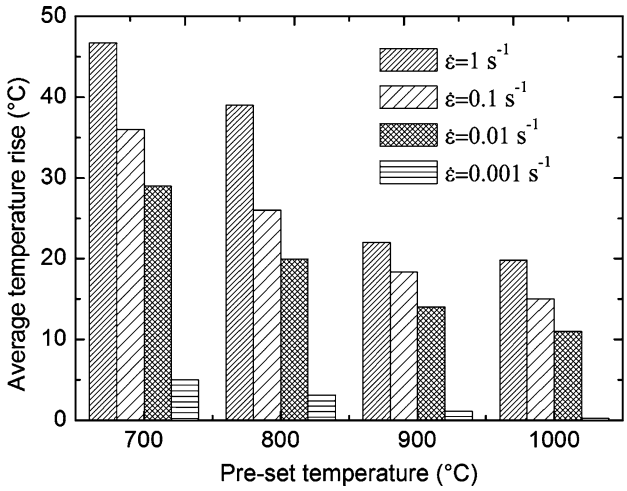

Fig. 4 Average temperature rise of the deformed cylinders at strain of 0.9 and different strain rates and temperatures

of the specimens is lower than the maximum temperature rise which is a clear indication of the temperature gradient in the deforming cylinder. At peripheral regions of the cylinder where the strain severity is not high the temperature rise is lower than the central region. The temperature gradient of a deforming sample at preset temperature of 700 °C and strain rate of 1 s^{-1} is also obvious in Fig. 5.

In order to find the value of flow stress at the absence of deformation heating the dependence of $\ln(\sigma)$ versus $10000/T$ (T denotes the average instantaneous temperature during the test) at each strain has been presented in Fig. 6. By reading the value of stress at a pre-set temperature, the change of flow stress due to temperature rise caused by deformation heating can be determined. It is worth noting that since constitutive Eq 7 is not dependent on strain, the plot of $\ln(\sigma)$ versus $10000/T$ should be made at each selected strain. Figure 7 represents the effect of deformation heating on the hot flow curves after correction. It can be seen that at low strain rates and high pre-set temperatures the effect of deformation heating on the flow

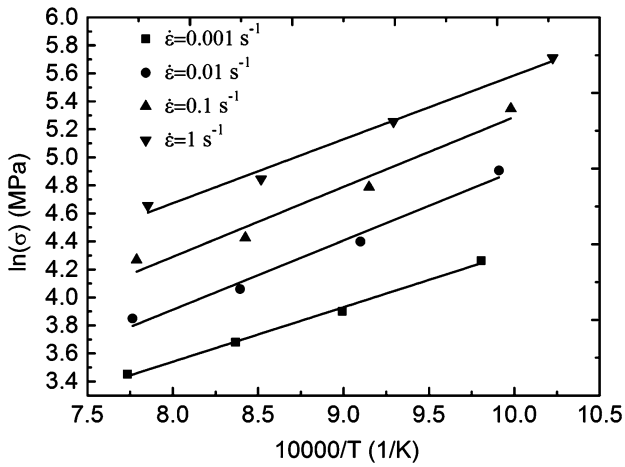

Fig. 6 Plot of $\ln(\sigma)$ versus $10000/T$. Note that T is the average instantaneous temperature of the deforming sample at each strain, i.e., $(T + 273 + \Delta T)$

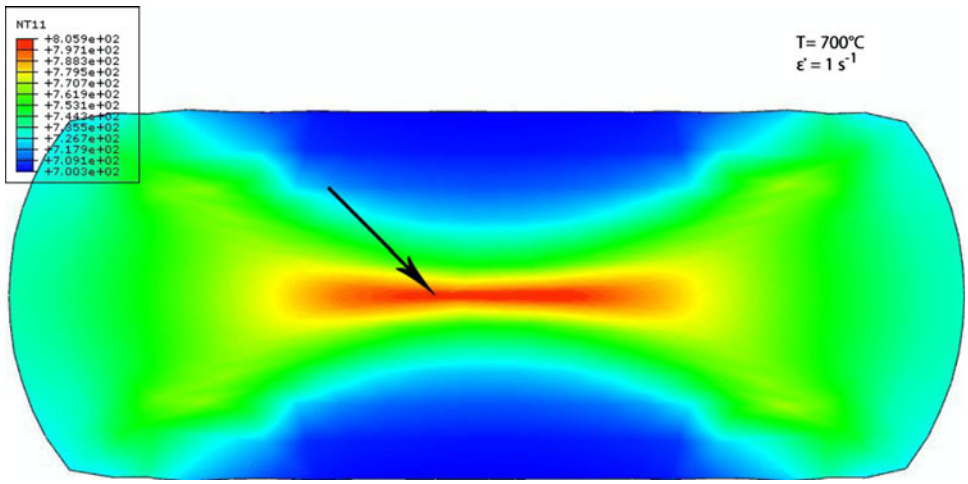

Fig. 5 Plot of Abaqus simulation demonstrating temperature gradient in the deforming sample

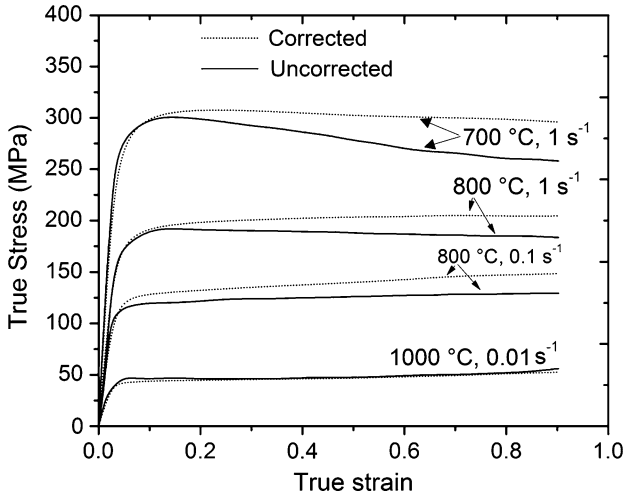

Fig. 7 Comparison between the corrected and the uncorrected flow curves. Note that the flow softening vanishes after the correction

curves is indeed insignificant. Further, the flow softening is no longer pronounced after correction of deformation heating implying dynamic recovery as a restoration mechanism in the equi-atomic NiTi.

With the corrected flow stress at each deformation strain, the functionality of the constitutive constants with strain in the form of Eq 7 can be obtained using the following polynomials:

$$n = -4.05\varepsilon^4 + 8.33\varepsilon^3 - 4.43\varepsilon^2 + 1.25\varepsilon + 5.85 \quad \text{(Eq 16)}$$

$$Q = -478.99\varepsilon^4 + 1029.53\varepsilon^3 - 805.71\varepsilon^2 + 313.73\varepsilon + 185.98 \quad \text{(Eq 17)}$$

$$\ln(A) = -18.77\varepsilon^4 + 38.57\varepsilon^3 - 38.2\varepsilon^2 + 17.44\varepsilon - 8.92 \quad \text{(Eq 18)}$$

Figure 8 presents the variation of the constants with strain prior and after correcting the effect of deformation heating. It is noted that the difference between the corrected and the uncorrected constants becomes more pronounced with the progress of deformation due to the more deformation heating effect. However, the activation energy of deformation does not show a significant alteration after the correction. Besides, the value of n increases from 5.9 to 7.38 before correction, while it increases from 5.9 to 6.82 for the corrected condition. It is of practical interest that the value of n decreases considerably as a result of correction of deformation heating. In another word, the flow behavior of equi-atomic NiTi after correcting the effect of deformation heating reveals larger values of m ($m = 1/n$) which is an indication of better workability. This phenomenon is most likely due to the thermal softening which is followed by flow localization, erases the stabilizing effect of work hardening leading to material instability as shown by Recht (Ref 21). Further, $\ln(A)$ has an increasing trend up to a strain of 0.4 and decreases with increasing the value of deformation strain. The value of activation energy increases from about 210 to 252.4 kJ/mol at strain of 0.9, indicating the difficulty of deformation. The activation energy of 210 kJ/mol at the beginning of plastic deformation, i.e., strain of 0.1, and the increasing trend obtained in this study is in agreement with those reported by Khamei et al (Ref 22) for a Ni-rich (60 wt.% Ni) NiTi alloy. Zhang et al. (Ref 23) reported an activation of

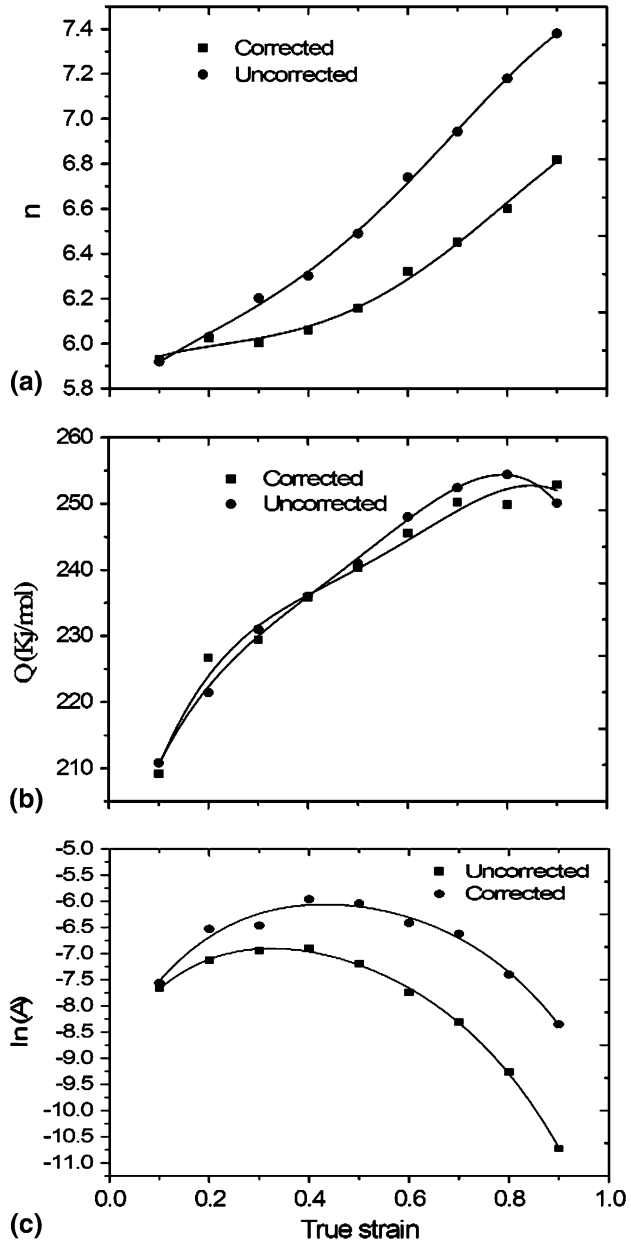

Fig. 8 Variation of constitutive constants with strain. (a) for n, (b) activation energy, and (c) $\ln(A)$

about 208 kJ/mol for NiTi alloy (50.7 wt.% Ni). However, they have reported a decreasing trend for the activation energy with increasing deformation strain. Researchers who have investigated on the creep behavior of NiTi alloys reported diverse values for the activation energy of the alloy (Ref 24). Among those studies, the reported values by Lexcellent et al. (Ref 25) and Mukherjee (Ref 26) who have reported the activation energies of 222 ± 30 and 251 ± 13 kJ/mol, respectively, are closer to the obtained values in this study confirming Ti diffusion in NiTi as the controlling mechanism of deformation. The observed inconsistency in the literatures related to the values of activation energy may be attributed to the difference in chemical composition, leading to precipitation mechanisms (formation and dissolution) being active at high temperatures. In NiTi alloys, a slight deviation from equi-atomic composition leads to a considerable precipitation (Ref 27) which changes the

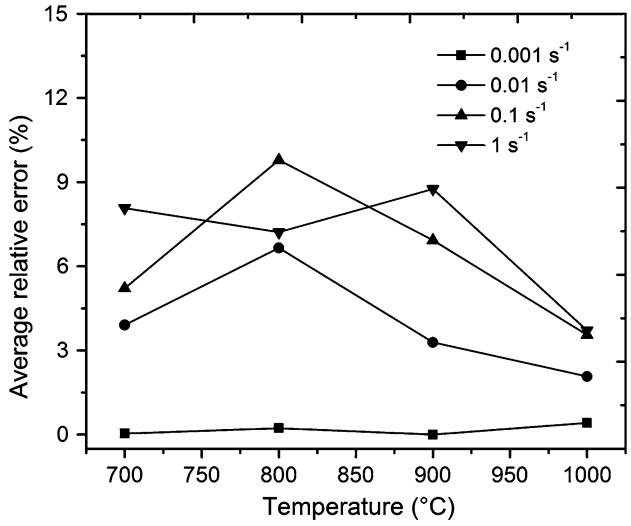

Fig. 9 Average relative error of flow stress due to the correction of deformation heating varying with temperature and strain rate

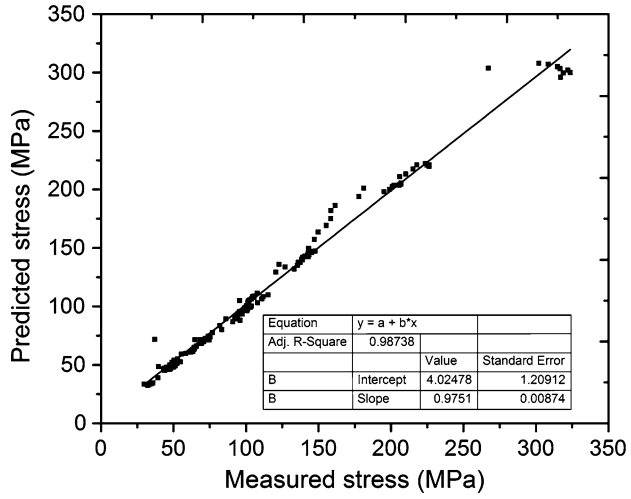

Fig. 10 Correlation between the fitted and measured flow stresses

ease of deformation during hot working. The decreasing trend in the activation energy reported in Ref 23 is very important in designing the hot working process of Ni-rich alloys and is likely be due to precipitation dissolution. Minimization of precipitates during hot working of a Ni-rich alloy has also been reported by Frick et al. (Ref 28). However, in this study, the alloy is highly close to equi-atomic composition (precipitate free) and formation or dissolution of precipitates seems not to be active during hot working.

In order to show the importance of the proposed correction the constitutive equation of equi-atomic NiTi, the relative error between the corrected and the uncorrected flow stresses was calculated using the following equation:

$$\text{Relative error} = \left| \frac{\sigma_{\text{Corr}} - \sigma_{\text{Uncorr}}}{\sigma_{\text{Corr}}} \right| \times 100 \qquad \text{(Eq 19)}$$

Figure 9 presents the average relative error over the strain range of 0.1-0.9 associated with the correction of deformation heating. From this figure one can notice that at low strain rates such as 0.001 s^{-1} the error is not significant. With increasing strain rate the relative error increases and it reaches up to about 9.5% at temperature of 800 °C and strain rate of 0.1 s^{-1}. The results indicate that deformation heating imposes considerable errors in the accuracy of the constitutive equation of equi-atomic NiTi alloy leading to erroneous results during numerical analysis of hot working. However, if the alloy is being hot worked at high temperatures such as 1000 °C with low strain rates, the correction is no longer necessary and the Eq 11-13 can satisfactorily be used to model the flow behavior during hot working.

Further, the accuracy of the corrected constitutive equation was evaluated by plotting the values of fitted flow stress versus measured flow stress and fitting a line throughout the points. According to Fig. 10, the R^2 regarding the line fitted for the fitted and the measured flow stresses of the equi-atomic NiTi is 98.738% implying an accuracy of near 99%. Therefore, the power-law constitutive equation in the form of Eq 7 and the dependency of its constants as a function of deformation strain can satisfactorily be employed to numerically model the hot working process of equi-atomic NiTi alloy under the similar condition.

7. Conclusions

In this study, the effect of deformation heating was eliminated from the hot flow curves of a near equi-atomic NiTi and a set of constitutive equation coupling flow stress with strain, strain rate, and temperature was proposed which has not been studied so far. The following conclusions can be drawn from this study:

1. At high strain rates and low pre-set temperatures the flow curves represent a flow softening, while, after correcting the effect of deformation heating, the flow softening vanishes.
2. The temperature of the deforming cylinder increases considerably at high strain rates. The average temperature reaches up to about 47 °C at temperature of 700 °C and strain rate of 1 s^{-1}.
3. The alloy constants, i.e., n, A, and Q in the constitutive equation are dependent on strain. The activation energy increases with increasing the deformation strain from about 210 up to 252 kJ/mol, indicating the difficulty of deformation.
4. The average relative error between the corrected and the uncorrected flow stress, over the whole strain range tested (0.1-0.9), showed the significant influence of the correction on the flow curves. The average relative error was about 9.5% at strain rate of 0.1 s^{-1} and temperature of 800 °C.

Acknowledgments

The authors would like to thank the Sharif University of Technology, Tehran, Iran for the financial support and provision of the research facilities used in this study.

References

1. T. Duerig, A. Pelton, and D. Stöckel, An Overview of Nitinol Medical Applications, *Mater. Sci. Eng. A*, 1999, **273**, p 149–160
2. D.C. Lagoudas, *Shape Memory Alloys Modeling and Engineering Applications*, 1st ed., Springer, 2008, p 30
3. M.H. Wu, Fabrication of Nitinol Materials and Components, *Mater. Sci. Forum*, 2002, **285**, p 394–395
4. L. Li, J. Zhou, and J. Duszczyk, Determination of Constitutive Relationship for AZ31B Alloy and Validation Through Comparison Between Simulated and Real Extrusion, *J. Mater. Process. Technol.*, 2006, **172**, p 372–380
5. A.K. Ghosh, On the Measurement of Strain-Rate Sensitivity for Deformation Mechanism in Conventional and Ultra-Fine Grain Alloys, *Mater. Sci. Eng. A*, 2007, **463**, p 36–40
6. R.L. Goetz and S.L. Semiatin, The Adiabatic Correction Factor for Deformation Heating During the Uniaxial Compression Test, *J. Mater. Eng. Perform.*, 2001, **10**, p 710–717
7. S. Bruschi, S. Poggio, F. Quadrini, and M.E. Tata, Workability of Ti-6Al-4V Alloy at High Temperatures and Strain Rates, *Mater. Lett.*, 2004, **58**, p 3622–3629
8. W. Zhang and S.H. Zhang, Correcting of Hot Compression Test and Constitutive Equation of NiTi, *Acta Metall. Sinica*, 2006, **42**, p 1036–1040 (in chinese)
9. D.C. Lagadous and Zh. Bo, Thermomechanical Modeling of Polycrystalline SMAs Under Cyclic Loading, Part II: Material Characterization and Experimental Results for a Stable Transformation Cycle, *Int. J. Eng. Sci.*, 1999, **37**, p 1141–1173
10. R. Hu, P. Nash, Q. Chen, L. Zhang, and Y. Du, Heat Capacities of Several Al-Ni-Ti Compounds, *Thermchim. Acta*, 2009, **486**, p 57–65
11. D.L. Baragar and A.F. Crawley, Frictional Effect on Flow Stress Determination at High Temperatures and Strain Rates, *J. Mech. Work Technol.*, 1984, **9**, p 291–299
12. M. Talebi Anaraki, M. Sanjari, and A. Akbarzadeh, Modeling of High Temperature Rheological Behavior of AZ61Mg-Alloy Using Inverse Method and ANN, *Mater. Des.*, 2008, **29**, p 1701–1708
13. R. Ebrahimi and A. Najafizadeh, A New Method for Evaluation of Friction in Bulk Metal Forming, *J. Mater. Process. Technol.*, 2004, **152**, p 136–143
14. H.J. McQueen and N.D. Ryan, Constitutive Analysis in Hot Working, *Mater. Sci. Eng. A*, 2002, **322**, p 43–63
15. M. Haghshenas, A. Zarei-Hanzaki, S.M. Fatemi-Varzaneh, and H. Abedi, Hot Deformation Behavior of Thixocast A356 Aluminum Alloy During Compression at Elevated Temperature, *Int. J. Mater. Form*, 2008, **1**, p 1001–1005
16. H.J. McQueen and C.A.C. Imbert, Dynamic Recrystallization: Plasticity Enhancing Structural Development, *J. Alloys Compd.*, 2004, **378**, p 35–43
17. A.R. Salehi and A. Karimi Taheri, Flow Behavior and Microstructural Evolution of 53Fe-26Ni-15Cr Superalloy During Hot Compression Test, *Ironmak Steelmak*, 2007, **34**, p 151–156
18. S. Serajzadeh, Development of Constitutive Equations for a High Carbon Steel Using Additivity Rule, *ISIJ. Int*, 2003, **43**, p 1050–1055
19. D. Yuan-Pei, L. Ping, X. Ke-min, Z. Qing, and W. Ziao-xi, Flow Behavior and Microstructure Evolution of TB8 Alloy During Hot Deformation Process, *Trans. Nonferrous Met. Soc. China*, 2007, **17**, p 1199–1204
20. P.L. Charpentier, B.C. Store, S.C. Ernest, and J.F. Thomas, Characterization and Modeling of the High Temperature Flow Behavior of Aluminum Alloy 2024, *Metall. Mater. Trans. A*, 1968, **17A**, p 2227–2237
21. R.F. Recht, Catastrophic Thermoplastic Shear, *J. Appl. Mech. Trans. ASME*, 1964, **31**, p 189–193
22. A.A. Khamei and K. Dehghani, Modeling the Hot-Deformation Behavior of Ni60wt%-Ti40%wt Intermetallic Alloy, *J. Alloys. Compd.*, 2010, **490**, p 377–381
23. H. Zhang, Y. HE, X. Liu, and J. Xie, Hot Deformation Behavior and Constitutive Relationship of Ni-Ti Shape Memory Alloy During Compression at Elevated Temperatures, *Acta Metall. Sinica*, 2007, **43**, p 930–936
24. S.M. Oppenheimer, A.R. Yung, and D.C. Dunand, Power-Law Creep in Equiatomic Nickel-Titanium Alloys, *Scripta Mater.*, 2007, **57**, p 377–380
25. C. Lexcellent, P. Robinet, J. Bernardini, D.L. Beke, and P. Olier, High Temperature Creep Measurements in Equi-Atomic NiTi Shape Memory Alloy, *Materialwiss. Werkst.*, 2005, **36**, p 509–512
26. A.K. Mukherjee, High-Temperature Creep Mechanism of NiTi, *J. Appl. Phys.*, 1968, **39**, p 2201–2204
27. K. Otsuka and X. Ren, Physical Metallurgy of Ti-Ni-Based Shape Memory Alloys, *Prog. Mater. Sci.*, 2005, **50**, p 511–678
28. C.P. Frick, A.M. Ortega, J. Tyber, K. Gall, and H.J. Maier, Multiscale Structure and Properties of Cast and Deformation Processed Polycrystalline NiTi Shape-Memory Alloys, *Metall. Mater. Trans. A*, 2004, **35**, p 2013–2025